Tech. Dig. Int. Elec. Dev. Mtg., pp. 607-610 (2000)

Improved External Coupling Efficiency in Organic Light-Emitting Devices on High-Index Substrates

M.-H. Lu, C. F. Madigan, and J. C. Sturm,
Center for Photonics and Optoelectronic Materials, Princeton University,
Princeton, NJ 08544, minhaolu@ee.princeton.edu

Abstract

High-index-of-refraction substrates are shown theoretically and experimentally to increase the external coupling efficiency of organic light-emitting devices (OLEDs) by using a quantum mechanical microcavity model. This increase is due to the elimination of those modes waveguided in the ITO/organic layer. Bi-layer OLEDs were fabricated on standard soda lime glass and high-index glass substrates, and their far-field intensity pattern was measured. Among the devices optimized for external efficiency, those on shaped high-index substrates exhibited a 53% improvement in external quantum efficiency over the devices on shaped standard glass substrates, and an increase by a factor of 2-3 times over those on planar glass substrates. This principle is applicable to any backside patterning technique in conjunction with other OLED structural improvements.

Introduction

A critical figure of merit of OLEDs is the external coupling efficiency (η_{ext}), defined as the ratio of photons externally emitted over photons generated. It is well known that a substantial amount of internally generated light is trapped in the high-index materials of the OLED stack (1), thus reducing η_{ext} to ~0.20-0.30 for typical structures. This commonly reduces the power efficiency of the OLEDs. Substrate patterning that recovers some of the trapped light has been shown to improve the OLED external coupling efficiency (2-4). In this work, we use shaped high-index substrates to further increase the amount of light that can be recovered.

The typical OLED consists of a multi-layer sandwich of a planar glass substrate (n_{glass1} = 1.51), a layer of indium-tin-oxide (ITO) (n_{ITO} = 1.8 – 2.0), one or more organic layers (n_{org} = 1.6 – 1.8), and a reflecting cathode. The emitted light can be classified into three modes: the external modes where the light escapes the substrate, the substrate-waveguided modes where the light is trapped in the glass substrate by total internal refraction (TIR) at the glass/air interface, and the ITO/organic-waveguided modes where the light is trapped by TIR at the ITO/glass interface (fig. 1a). By patterning the backside of the glass substrate opposite to the OLED, some light in the substrate-waveguided modes can be made to emit externally (3, 4). However, the light in the ITO/organic-waveguided modes is not recoverable by this technique. By using high-index substrates (n_{glass2} = 1.85 > n_{org}), the ITO/organic modes can be eliminated. Thus leaving more light available for conversion into external modes (fig. 1b). Quantification of the light emitted into these different modes for different substrates and experimental verification is the purpose of this paper.

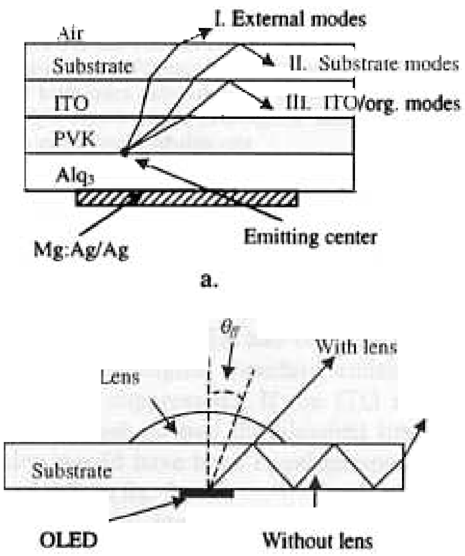

Fig. 1a. Three radiative modes in OLEDs: I. External modes, II. Substrate modes, and III. ITO/organic modes. b. Attaching a lens to the backside of OLED converts some light from substrate modes to external modes.[4]

Modeling

Since the layers in a typical OLED are much thinner than the emission wavelength, external coupling of light is poorly described by classical ray optics. A quantum mechanical microcavity theory of OLEDs developed by Bulovic et al. (5) has been used to calculate the distribution of light emission into various modes and to predict the amount of increase in external emission by attaching a lens to the backside of the substrate (7). In this formulation, the exciton is modeled as a radiating dipole, and the external coupling efficiency is proportional to the transition rate given by Fermi's golden rule:

$$f = \frac{2\pi}{h} \sum_n \left| \langle m | \mathbf{\mu} \cdot \mathbf{E}(\mathbf{k}, z) | n \rangle \right|^2 \delta(E_n - E_m - h\upsilon) \qquad (1)$$

where $\boldsymbol{\mu}$ is the dipole moment which is assumed to be isotropically distributed, and $\mathbf{E}(\mathbf{k}, z)$ is the electrical field for mode $\mathbf{k}$ at the dipole. E_m and E_n are the energies of the initial and final exciton states. $h\upsilon$ is the energy of the photon emitted. The transition rate is obtained by summing over all $\mathbf{k}$ and υ. The electric field for TE and TM modes at a distance l from the cathode is determined by the microcavity structure:

$$\begin{aligned} \mathbf{E}_{\mathbf{k}}^{TE} &= \mathbf{A}(\mathbf{k})\sin^2(k_{oz}l)\hat{\mathbf{x}} \\ \mathbf{E}_{\mathbf{k}}^{TM} &= \mathbf{B}(\mathbf{k})\cos^2\theta_o \operatorname{Sin}^2(k_{oz}l)\hat{\mathbf{y}} + \mathbf{C}(\mathbf{k})\sin^2\theta_o\cos^2(k_{oz}l)\hat{\mathbf{z}} \end{aligned} \qquad (2)$$

where $\mathbf{A}(\mathbf{k})$, $\mathbf{B}(\mathbf{k})$ and $\mathbf{C}(\mathbf{k})$ are functions of material constants and $\mathbf{k}$. k_{oz} is the z component of the wave vector in the emitting layer, and θ_o is the angle of the wave vector in the emitting layer measured from the normal. For spontaneous emission, the electrical fields are normalized such that the energy in each mode is equal to that of a single photon. In our devices (fig. 2), the excitons were assumed to be created at the Alq_3/PVK interface and diffuse into Alq_3 with a characteristic length of 20 nm (6). The transition rate into each optical mode was computed by integrating over photon energy and exciton location. Energy transfer to the cathode was approximated with the results given by Bulovic et al. (5).

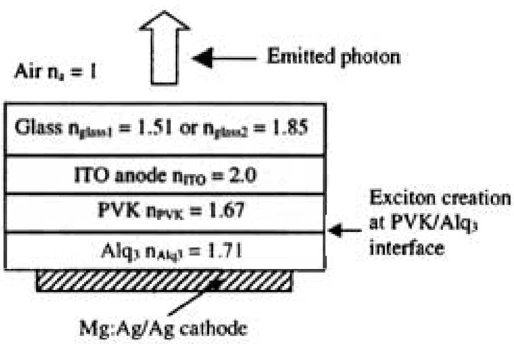

Fig. 2 Schematic diagram of OLEDs fabricated on standard (n = 1.51) and high-index (n = 1.85) glass substrates. Excitons are created at the PVK/Alq_3 interface. The location of the emission centers was controlled by the thickness of the Alq_3 layer, which was varied from 20 – 80 nm. External coupling efficiency depends critically on this distance.[4]

The amount of light emitted into external, substrate and ITO/org. modes in OLEDs on either the standard or high-index glass substrates was calculated using the QM microcavity model. Fig. 3 shows the detailed distribution of OLEDs with an 80 nm Alq_3 layer on both types of substrates. The external emissions are equal for the two devices, as this fraction is not dependent on the index of refraction of the intervening layers. In the device on high index substrates, light is no longer bounded by TIR at the glass/ITO interface and the ITO/organic modes are eliminated, while these modes remain in the device on standard substrates.

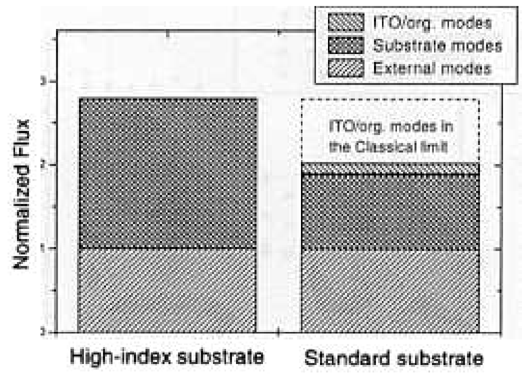

Fig. 3 Calculated distribution of emitted light into external, substrate and ITO/organic modes for OLEDs with 80 nm Alq_3, 40 nm PVK and 100 nm ITO on both high-index and standard substrates. ITO/organic modes are eliminated in the case of high-index substrates. In devices on standard substrates, QM effects on the ITO/organic modes lead to a suppression of the total emission rate.

Furthermore, since the thickness of the ITO and organic layers is much less than the wavelength in question, QM effects dominate such that the emission into the ITO/organic modes depends critically on the number of the modes. In our structure, there are at most one TE and one TM mode in the range of the visible wavelengths; therefore, emission into the ITO/organic modes is suppressed. If the ITO and organic layers were thick enough so that the classical limit applies, the total emission would have been equal irrespective of the substrate (dashed part in fig. 3).

Substrate patterning converts light trapped in the substrate modes into externally emitted light. Consequently, increased emission into substrate modes in OLEDs on high-index substrates allows more light to be harvested via substrate patterning. We calculated the expected increase in

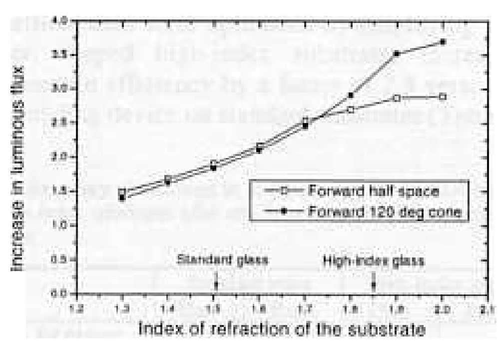

Fig. 4 Predicted increases in luminous flux emitted in the forward half plane and the forward 120° cone as a function of the index of refraction of the substrate, assuming complete conversion of substrate modes into external modes.

the external luminous flux by attaching a lens with the same index as the substrate, assuming a lens large enough that all light previously trapped in the substrate can be emitted externally (fig. 4). The predicted enhancement factor increases monotonically with the index of refraction of the substrate. As the index of the substrate increases beyond that of the emitting layer (n_{Alq3} = 1.71), emission becomes more concentrated in the forward direction due to refraction. Hence there is a larger factor of increase for the luminous flux in the forward 120° cone compared with that in the entire forward half space for higher substrate indices.

Experimental

Bi-layer OLEDs were fabricated on 0.5 mm-thick soda lime (n_{glass1} = 1.51) and high-index (Schott SF9 glass, n_{glass2} = 1.85) glass substrates. 100 nm of indium-tin-oxide (ITO, n_{ITO} = 2.0) was deposited onto both substrates by RF magnetron sputtering without intentional heating. The sheet resistance of the ITO was 100 Ω/sq, and the transmission was ~80% in the visible. The hole transport layer in all devices was a 40 nm layer of poly-(N-vinylcarbazole) (PVK, n_{PVK} = 1.67), deposited by spin-coating after the ITO surface was treated by an O_2 plasma (8). The electron transport and emitting layer in all devices was tris-(8-hydroxyquinoline)aluminum (Alq_3, n_{Alq} = 1.71), deposited by vacuum sublimation. The cathodes were 30 nm of Mg:Ag (10:1) followed by an Ag cap evaporated through a shadow mask with 0.5 mm-diameter holes. The EL spectrum showed that light emission was exclusively from the Alq_3 layer. The lenses used in this experiment were made from the same material as the substrates. All lenses have a radius of curvature of 2.0 mm and a height of 1.5 mm, placing the OLED exactly at the center of the curvature. Index matching oil (n_{oil1} = 1.51) and gem refractometer liquid (n_{oil2} = 1.81, both from R.P. Cargille Lab. Inc.) were used to match the lenses to their respective substrates. The far-field emission pattern was measured by a Si photo-detector with a linear polarizer.

Data and Discussion

Fig. 5 shows the far-field intensity pattern of an OLED with an 80 nm Alq_3 layer on both standard and high-index substrates, with and without a lens attached. As expected, in devices fabricated on planar substrates, the far-field intensity patterns are the same, irrespective of the index of the substrates. Once a lens of the same index as the substrate is attached, the devices on the high-index substrates showed an average increase by a factor of 3.2 in the intensity in the normal direction versus an average increase by a factor of 2.2 for the devices on the standard substrates. These results are very close to the ideal scenario where the OLED is a point source at the center of curvature of the lens where the expected increase is given by n_{glass}^2, i.e., by factors of 3.4 and 2.3 for high-index and standard glass substrates respectively.

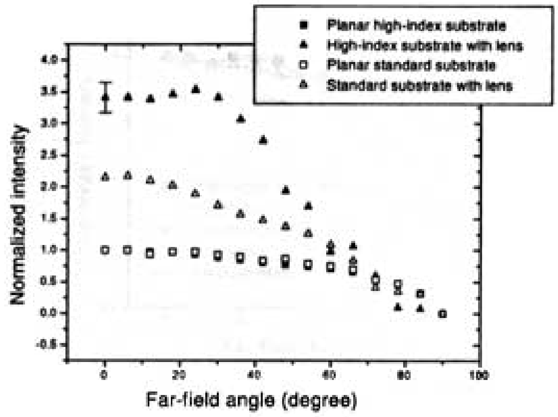

Fig. 5 Far-field intensity profile of an OLED (ITO/PVK/Alq_3 (80 nm)/Mg:Ag/Ag) on both high-index and standard glass substrates, before and after lens attachment.

When the far-field intensity was integrated to give the total external luminous flux, OLEDs on shaped high-index glass substrates showed significantly larger increases than those on standard glass substrates for all thicknesses of Alq_3 layers examined (20 – 80 nm). Due to microcavity effects, the far-field intensity pattern is not Lambertian. In devices with emission zones close to the cathode (i.e., with a thin Alq_3 layer), in-plane (large mode angle) TM radiation is enhanced with respect to radiation along the normal direction (5). As a result, a larger fraction of light emission suffers from TIR at the glass/air interface and becomes trapped in the substrate. Consequently, we expect a larger increase in externally emitted light by our substrate mode conversion technique in devices with thinner Alq_3 layers. This is confirmed by our data. The largest such increase observed was in a 20 nm Alq_3 device on high-index substrate, where the external quantum efficiency was increased by a factor of 2.7, versus an increase of 2.2 times for the corresponding device on standard substrates. In OLEDs whose initial quantum efficiencies were optimized by employing a 80 nm Alq_3 layer, shaped high-index substrates increased the external quantum efficiency by a factor of 2.3 versus 1.5 for the corresponding device on standard substrates (Table 1).

Table 1 Summary of increases in luminous flux for OLEDs on standard and high-index substrates after attaching a lens to the backside of the substrate.

	Standard glass		High-index glass	
	Theo.	Expt.	Theo.	Expt.
Q.E. for planar device[a]	N/A	0.35%	N/A	0.36%
Flux increase in forward half-space	1.82X	1.5X	2.62X	2.3X
Flux increase in forward 120° cone	1.82X	1.7X	3.20X	2.9X

[a] Quantum efficiency (external photon/electron) is the same for both types of devices as measured from a group of large-area planar OLEDs.

High-index substrates not only eliminate the ITO/organic modes, but also have a focusing effect on the distribution of emitted light rays. With a large substrate index (n_{glass2} = 1.85), diffraction from the emitting layer (n_{Alq3} = 1.71) bends light rays forward in the substrate. In the ideal scenario where the OLED is a point source at the center of the curvature of the lens, the far-field intensity pattern in air is identical to the ray distribution in the substrate, so the emission in air is also more concentrated in the normal direction. Thus if we were to look at the light emission in the forward 120° cone, where most of the viewing takes place, the amount of increase in external quantum efficiency is even more remarkable. The observed maximum increase was by a factor of 3.2 for a 20 nm Alq_3 OLED, and a factor of 2.9 for an 80 nm Alq_3 OLED, compared with factors of 2.6 and 1.7 for corresponding devices on standard substrates (Table 1). The discrepancy between theoretical and experimental values can be attributed to the finite size of the OLEDs and the imperfections at the edge of the lenses.

Above we calculated that the external emission amounts to 35.7% of total emission in the OLED on high-index substrates (fig. 3), which is much larger than the ~20% commonly assumed (1). To verify this result we correlated the reduction in the substrate-waveguided light with the increase in external emission after the lens was added. This was accomplished by measuring the normal and edge emission simultaneously. Because the ITO/organic modes are heavily attenuated by the electrodes (5), we assume that the edge emission consists of the substrate-waveguided light exclusively. Further, the total emission rate is assumed to be unchanged from the attachment of a lens on the backside of the substrate. This is reasonable given that the thickness of the substrate, 0.5 mm, was much larger than the wavelength in question. The ratio of emission into the external modes over that into the substrate modes can be calculated from the change in the external and edge emission before and after adding a lens (7). For an OLED with 80 nm Alq_3 on high-index substrate, the data implied an external modes/substrate modes ratio of 0.40 ± 0.08, whereas the ratio in a corresponding device on standard substrate was found to be 1.30 ± 0.30. From the calculations presented in fig. 3 we expect this ratio to be 0.56 and 1.12 for devices on high-index and standard substrates respectively, so the agreement between theory and experiment is very good considering the large error associated with the measurement.

Increased light emission into the substrate modes can be further demonstrated by a more practical substrate modification technique. When OLEDs were fabricated on substrates whose backsides were roughened by abrasion (resulting RMS roughness = 75 nm in both cases as measured by a profilometer). Light in the substrate modes was partially scattered forward. Fig. 6 shows the far-field intensity profile of the resulting OLEDs. The OLED on the high-index substrate exhibited a 39% increase in total external emission compared with a 17% increase for the OLED on the standard substrate. Again, this is consistent with the numerical results

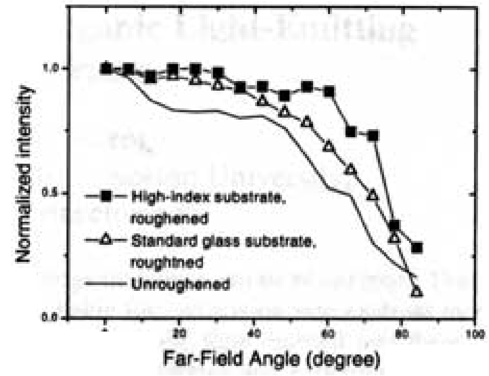

Fig. 6 Far-field intensity of OLEDs with roughened backside. Total luminous flux from the OLED on a high-index substrate was increased by 39% as compared with the unroughened sample; the increase for the OLED on a standard glass substrate was only 17%. Roughening the backside does not change the intensity in the normal direction.

presented in fig. 3, where emission into substrate modes in the device on high-index substrates is roughly twice that of the corresponding device on standard substrates.

Conclusions

We have demonstrated both theoretically and experimentally that shaped high index of refraction substrates enhances external coupling efficiency by eliminating ITO/organic waveguided modes and redirecting them externally. Using this process, a 2-3-fold increase in the external quantum efficiency of the OLED can be achieved.

References

N. C. Greenham, R. H. Friend, and D. D. C. Bradley, "Angular dependence of the emission from a conjugated polymer light-emitting diode: implications for efficiency calculations", *Adv. Mater.*, vol. 6, pp. 491-494, 1994.

2. G. Gu, D. Z. Garbuzov, P. E. Burrows, S. Venkatesh, and S. R. Forrest, "High-external-quantum-efficiency organic light-emitting devices", *Opt. Lett.*, vol. 22, pp. 396-398, 1997.
3. T. Yamasaki, K. Sumioka, and T. Tsutsui, "Organic light-emitting device with an ordered monolayer of silica microspheres as a scattering medium", *App. Phys. Lett.*, vol. 76, pp. 1243-1245, 2000.
4. C. F. Madigan, M.-H. Lu, and J. C. Sturm, "Improvement of output coupling efficiency of organic light-emitting diodes by backside substrate modification", *App. Phys. Lett.*, vol. 76, pp. 1650-1652, 2000.
5. V. Bulovic, V. B. Khalfin, G. Gu, and P. E. Burrows, D. Z. Garbuzov, and S. R. Forrest, "Weak microcavity effects in organic light-emitting devices", *Phys. Rev. B*, vol. 58, pp. 3730-3740, 1998.
6. C. W. Tang, S. A. VanSlyke, and C. H. Chen, "Electroluminescence of doped organic thin films", *J. Appl. Phys.*, vol. 65, pp.3610-3616, 1989.
7. M.-H. Lu, C. F. Madigan, and J. C. Sturm, "Experiment and modeling of conversion of substrate-waveguided modes to surface-emitted light by substrate patterning", *Mat. Res. Soc. Proc.* vol. 621, Q3.7, 2000.
8. C.-C. Wu, C.-I. Wu, J. C. Sturm, and A. Khan, "Surface modification of indium tin oxide by plasma treatment: an effective method to improve the efficiency, brightness and reliability of organic light emitting devices", *Appl. Phys. Lett.*, vol. 70, pp. 1348-1350, 1997.